Optical confinement in GaN based quantum dot embedded heterostructure

UJWALA ZOPE, E. P. SAMUEL, D. S. PATIL[*]
Department of Electronics, North Maharashtra University, Jalgaon [Maharashtra], India

Analysis of optical confinement in quantum dot embedded heterostructure has been carried out for the optimization of smaller active region volume to achieve desired modal gain. Overall optical confinement has been deduced by taking product of lateral, transverse and longitudinal optical confinements. Near field intensity distribution has been obtained to have clear insight of 3D fundamental electric mode confinement at 375 nanometer wavelength. Far field intensity reveals divergence of 26 degrees. Overall confinement shows nonlinear variation with quantum dot size. The near field confinement within the quantum dot seems to be excellent. Investigation of near, far field and optical confinement has been carried out with change in Aluminum mole fraction and dot dimensions.

1. Introduction

Semiconductor alloys and heterostructures based on the group III-nitride material system have received significant attention because of their potential application for the production of efficient optoelectronics devices. Gallium Nitride (GaN) based material system is the most promising [1–4] due to its wide emission capability from blue to ultraviolet wavelength region of electromagnetic spectrum. The large direct band gap of this material makes it highly attractive for optoelectronics, microelectronics and power electronics applications. In particular, blue light emitting GaN semiconductor light sources have great impact on industrial applications such as blue light emitting diodes and edge emitting lasers for application to displays, traffic signals and DVD. For the realization of short-wavelength lasers, theoretical [5-7] and experimental [8-9] research into GaN and related materials has been conducted intensively by many research groups.

Reducing dimensionality of the active region improves significantly the performance of semiconductor lasers. If one makes a heterostructure with sufficiently thin layers, quantum interference effects begin to appear prominently in the motion of the electrons. The simplest structure is a quantum well, which simply consists of a thin layer of a narrower-gap semiconductor between thicker layers of a wider-gap material. When the motion of a charge carrier in a crystal is limited to a very small volume the energy spectrum of the charge carrier is quantized. Quantum well [7] heterostructure are key components of many optoelectronic devices, because they can increase the strength of electro-optical interactions by confining the carriers to small regions. Once carriers are captured into this well [6], the probability to escape from the well is limited. Lasers with an active layer of InGaN quantum wells have been demonstrated at room temperature under continuous-wave and pulsed operation [3].

Further enhancement of device characteristics is expected for lasers with still lower dimensionality structure of quantum dot (QD) lasers [10-14]. Quantum well has a continuous density of states, while QD energy spectrum consists of discrete energy levels. QD lasers have been predicted to have superior thermal stability to conventional quantum well lasers. The reduction of threshold current due to the QD effect can be more enhanced in wider bandgap semiconductors, and, therefore, the use of the QDs in GaN-based lasers is very effective. Low threshold current can be achieved by simply making the active volume small [15]. Since, to be precise, when the volume is too small, necessary gain for lasing action can not be obtained, careful optimization of the active volume is needed. Three-dimensional (3-D) confinement in QD's naturally provides the desired lateral carrier confinement. The dot size variation only needs to be sufficiently small to provide enough gain for lasing at lower QD states. Besides this, QDs have smaller optical confinement factor, due to a reduced physical volume of the active region compared with typical quantum wells, and thus, the modal gain is reduced. Active region gain and differential gain are proportional to the optical confinement factor, which is the fraction of the optical mode power in the active region. The confinement factor [16] must be optimized for best laser performance by careful modeling of laser optical mode profile. Therefore, careful optimization of active region volume and the optical confinement is important to achieve the desired modal gain in QD heterostructure.

The main goal of this paper is to optimize quantum dot embedded heterostructure for its better optical confinement with its small size quantum dot. We have carried out optimization of near field intensity to confine

fundamental transverse electric mode at the center of the quantum dot. Far field intensity analysis has been carried out to determine the divergence angle. Overall optical confinement has been deduced by combining confinements in all three directions. Following section of paper describes the mathematical approach used for the analysis. Section 3 discusses significant results of near, far field and optical confinement. Finally, conclusions are highlighted.

2. Mathematical approach

Near field and far field are two of the significant issues concerning emitted optical field. Near field shows spatial intensity distribution of the emitted light near the wave-guide end face while the angular intensity distribution far from the end face is known as the far field. We have already carried out near field intensity analysis recently for GaN based channel substrate planar laser diode [5].
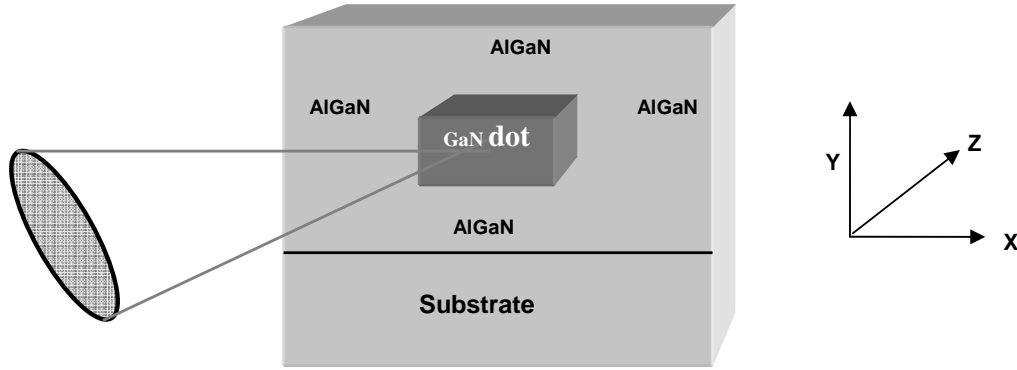

Fig. 1. Quantum dot embedded heterostructure.

Heterostructure with a cubic quantum dot (GaN) of 5 nanometer size has been embedded in AlGaN cladding material from all the sides as shown in Fig. 1. For the analysis of quantum dot embedded heterostructure, waveguide theory [16] has been used to investigate guiding effects along lateral, transverse and longitudinal directions. Spatial distribution of the optical field E(x,y,z) has been obtained for the fundamental electric mode by solving the wave equation expressed as follows:

$$\nabla^2 E + \left(k_0^2 n_r^2 - \beta^2\right) E = 0 \qquad (1)$$

Where, β is the mode propagation constant, k_0 is the free space propagation constant at 375 nanometer wavelength and n_r is the refractive index.

Three-layer wave-guide model is applied to quantum dot embedded heterostructure to compute optical field components and effective index method is used to deduce value of effective refractive index. The spatial distribution of the optical field associated with the transverse mode E(y) can be obtained from above wave equation and boundary conditions as follows:

$$\begin{aligned}
E(y) &= C e^{-py} \\
E(y) &= A \cos(qy) + B \sin(qy) \\
E(y) &= D e^{ry}
\end{aligned} \qquad (2)$$

Where, A, B, C and D are arbitrary constants and p, q and r are wave numbers.

In the similar manner field components have been obtained for lateral and longitudinal directions. Near Field intensity [5] has been computed in each region from exact field solutions in which effective refractive index N has been computed using effective index method. The spread in the field has been obtained and optical confinement factor has been deduced to optimize active region volume of the heterostructure.

Far field is important in determining the divergence and coupling efficiency. Writing E in equation (1) in terms of plane waves by Fourier transform theory

$$\psi(s) = 1.0 / \left(\sqrt{2\pi}\right) \int_{-\infty}^{\infty} E(y) \exp(isy) dy \qquad (3)$$

where, s is propagation constant along x-direction.

Consider the co-ordinate system in which

$$x = r \sin \theta \qquad (4)$$

$$z = r \cos \theta \qquad (5)$$

$$s = k_0 \sin \phi \qquad (6)$$

$$ds = k_0 \cos \phi d\phi \qquad (7)$$

Mathematically, taking the Fourier transform of the near field one can approximate the far-field intensity distribution as

$$I(\theta) = E(r,\theta)^2$$
$$I(\theta) = I_0 * |\psi|^2 * g(\theta)^2 \tag{8}$$

At this juncture, I_0 is peak near field intensity value at the center of active region, $|\psi|$ is Fourier transform of near field E_y, and $g(\theta)$ is the coefficient to combine all the $\cos(\theta)$ terms in the structure.

$$g(\theta) = 2\cos(\theta) * [(\beta / k_0) + \sqrt{(N^2 - \sin^2\theta)}] / [\cos(\theta) + $$
$$+ \sqrt{(N^2 - \sin^2\theta)}] \tag{9}$$

At this point, θ is the angle, β is the mode propagation constant, and k_0 is the free space propagation constant.

Overall optical confinement factor has been considered as a product of the lateral, transverse and longitudinal confinement factors as follows:

$$\Gamma = \frac{\int_{active} E^2 dy}{\int_{-\infty}^{+\infty} E^2 dy} = \Gamma_x . \Gamma_y . \Gamma_z \tag{10}$$

with, $\quad \Gamma_x = \dfrac{\int_w E_x^2 dx}{\int_x E_x^2 dx}$

$$\Gamma_y = \frac{\int_d E_y^2 dx}{\int_y E_y^2 dx}$$

$$\Gamma_z = \frac{\int_L E_z^2 dx}{\int_L E_z^2 dx}$$

The value of Γ_z is considered to be unity since the active region spans the entire length of the waveguide.

3. Results and discussion

Significant results of lateral (X-direction), transverse (Y-direction) and overall confinement in GaN quantum dot embedded heterostructure have been presented here for the near field intensity. The value of the near field intensity has been obtained by squaring the field amplitudes, which have been obtained from the solutions of wave equation. Fig. 2 illustrates the 3D near field intensity distribution in active volume of quantum dot at 375 nanometers wavelength. The dot thickness of 5 nanometers and Aluminum mole fraction 0.3 has been considered for this analysis. The near field intensity shows a sharp confinement at the center of the dot region. The confinement of the near field intensity in the quantum dot region is due to the refractive index variation of the quantum dot region (GaN) and the cladding region of AlGaN around the dot. The spread of the near field

intensity observed in the cladding region is due to the tunneling of optical field that occurs due to the very small volume of the quantum dot. Refractive index of active volume and cladding were considered to be 2.5623 and 2.3853 respectively, which provides effective index of 2.3856.
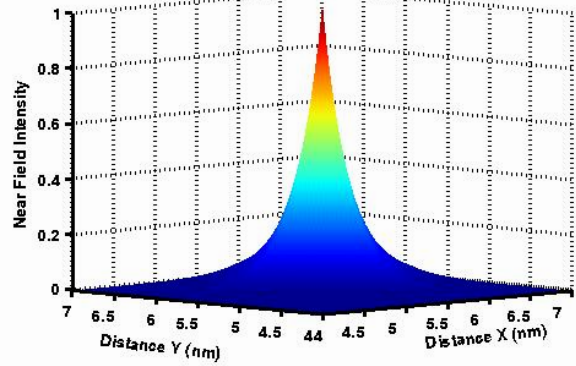

Fig. 2. 3D confinement of near field at 375-nanometer wavelength.

Fig. 3 illustrates spreading of near field intensity with Aluminum mole fraction. The full width at half maximum (FWHM) of the relative intensity has been investigated as a function of Aluminum mole fraction considering 5 nanometer dot thickness. It was obtained from our analysis that FWHM decreases nonlinearly with increase of Aluminum mole fraction. It clearly indicates that the field is confined more within the active layer with less extent in barrier layer for the increasing values of Aluminum mole fraction. The value of FWHM deduced from our analysis was 1.929 micrometers for 15 % of Aluminum mole fraction and get reduced to 1.021 micrometers for 30 % Aluminum mole fraction.
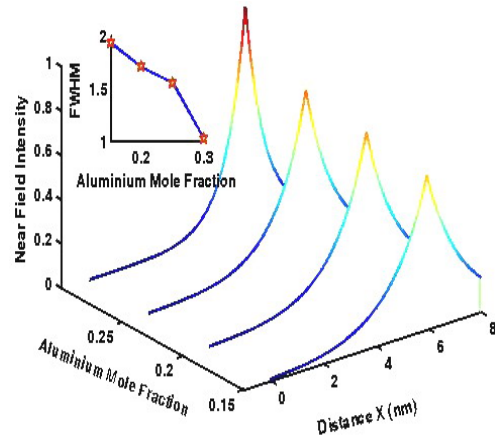

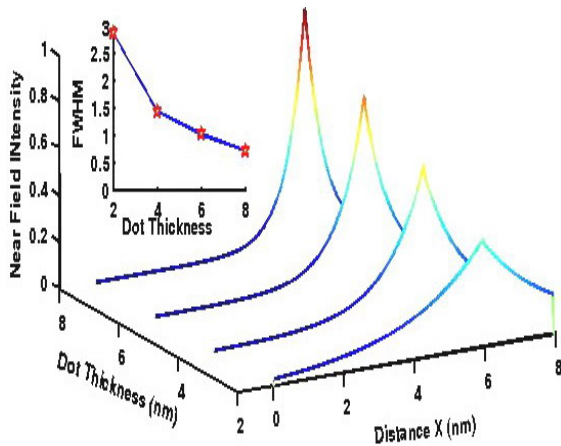*Fig. 3. Near field intensity as a function of Aluminum mole fraction.*

Fig. 4. Effect of dot thickness on near field at 375-nanometer wavelength.

The effect of spread of relative field intensity around center of active layer was analyzed at 375 nanometer wavelength as shown in Fig. 4 for varying quantum dot thickness by assuming 30 % Aluminum mole fraction. The full width of half maximum (FWHM) of the relative intensity has been investigated as a function of dot thickness. It was realized from our analysis that FWHM decreases nonlinearly with increase of Aluminum mole fraction in the barrier layer. It clearly indicates that the field is confined more within the active layer with less extent in barrier layer for 8-nanometer dot thickness. The value of FWHM deduced from our analysis was 2.882 micron for 2-nanometer dot thickness and get reduced to 0.726 micron for 8-nanometer dot thickness.
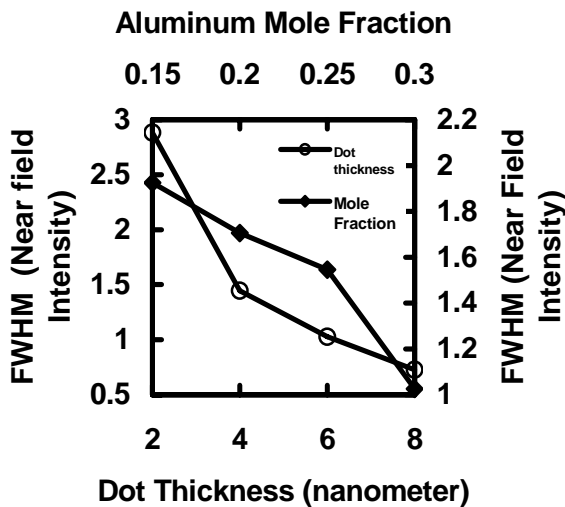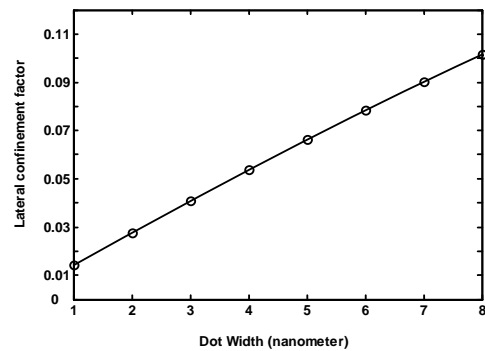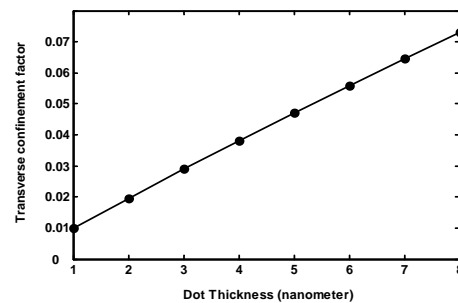

Fig. 5. FWHM (degree) of near field intensity as a function of dot thickness and Aluminum mole fraction.

Fig. 5 explains full width of half maximum (FWHM) of near filed intensity as a function of dot thickness and
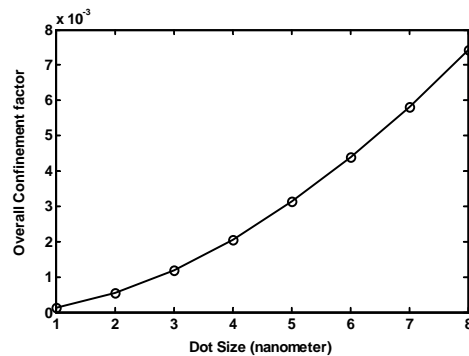
Aluminum mole fraction. FWHM decreases with increase in dot thickness considering 30% Aluminum mole fraction. The value of FWHM deduced from our analysis was 2.882 micrometers for 2-nanometer dot thickness and get reduced to 0.726 micrometers for 8-nanometer dot thickness. The value of FWHM decreases with increase in Aluminum mole fraction considering dot thickness of 5 nanometers. The value of FWHM deduced from our analysis was 1.929 micrometers for 15 % of Aluminum mole fraction and get reduced to 1.021 micron for 30 % Aluminum mole fraction. It clearly indicates that optical field confinement enhances with increase of Aluminum mole fraction and dot thickness. This has been attributed to the increase in refractive index step between active region and cladding layers along with increase of active region volume.

a

b

c

Fig. 6. Optical confinement factor (a) Lateral, (b) Transverse, (c) Overall.

The confinement factor which shows fraction of field intensity confined within active volume out of total intensity was calculated as a function of dot dimensions as demonstrated in Fig. 6. Lateral confinement along X-direction increases from 0.013 to 0.1 with increase of dot width from 1 to 8 nanometers. The variation of lateral optical confinement factor is linear due to small variation of dot width compared to overall dimensions of quantum dot heterostructure. Value of 2.3857 was deduced at 375 nanometer wavelength for effective refractive index using effective index method. Transverse confinement factor shows variation from 0.01 to 0.073 with increase of dot thickness from 1 nanometer to 8-nanometer. Overall confinement factor has been estimated as a function of active region volume by taking product of lateral, transverse and longitudinal confinement factors. Overall confinement factor shows nonlinear variation with dot dimensions.
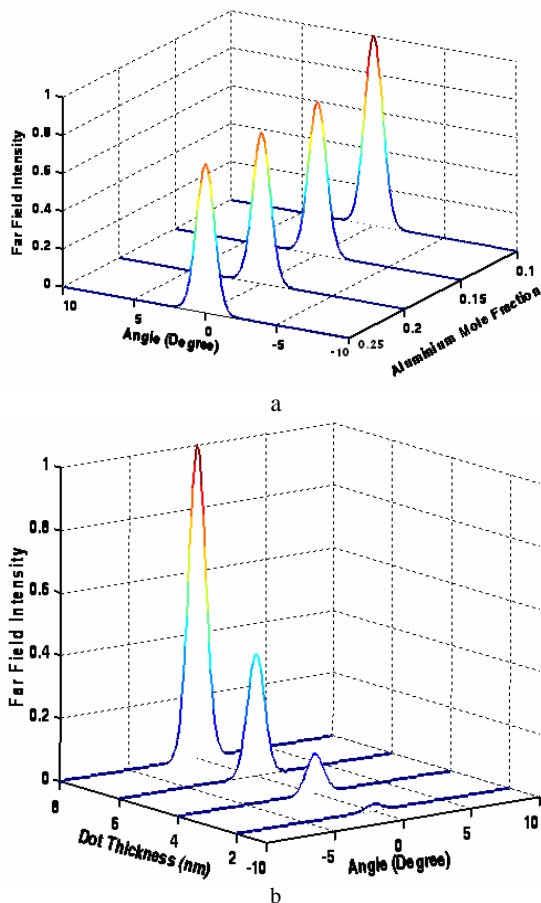
intensity goes on decreasing. This is due to dominant value of near field intensity at the center of active region for the lower values of mole fraction. The spread of far field intensity with dot thickness has been investigated as shown in Fig. 7 (b). It was observed that far field intensity is greater for higher values of dot thickness which has been attributed to better confinement of optical field in increased active region volume. The divergence angle (2θ) was found to be 26 degrees.

4. Conclusions

The analysis of quantum dot (GaN) embedded heterostructure at 375-nanometer wavelength has been carried for optimizing the active region volume and optical confinement which affects the modal gain. The lateral, transverse and overall confinement factor was deduced as a function of dot dimensions. However, overall confinement factor increases nonlinearly with increase in dot dimensions. Near field intensity distribution shows its peak value exactly at the center of the quantum dot. Far field intensity has been investigated as a function of Aluminum mole fraction and dot thickness. It reveals its maximum value for the greater values of dot thickness. Divergence of 26 degrees was deduced from the far field analysis. Our analysis is significant for exploring optimization of optical confinement along with quantum confinement to improve performance of quantum dot lasers.

a

b

Fig. 7. Far field intensity as a function of (a) Aluminum mole fraction, (b) dot thickness.

The variation of far field intensity with angle for different values of Aluminum mole fractions is explained in Fig. 7 (a). It was found from our analysis that for 10 % mole fraction, relative far field intensity shows dominant peak. However, as we increase mole fraction, far field

References

[1] W. Lu, D. B. Li, C. R. Li, F. Shen, Z. Zhang, J. Appl. Phys. **95**, 4362 (2004).

[2] I. Vurgaftman, J. R. Meyer, L. R. Ram-Mohan, Journal of Applied Physics **89,** 5815 (2001)**.**

[3] S. Nakamura, M. Senoh, S. Nagahama, T. Matsushita, H. Kiyoku, Y. Sugimoto, T. Kozaki, H. Umemoto, M. Sano, T. Mukai, Jap. Journal of Applied Physics **38**, L226 (1999).

[4] V. Darakchieva, E. Valcheva, P. P. Paskov, M. Schubert, T. Paskova, B. Monemar, H. Amano and I. Akasaki, Physical Review B **71**, 115329 (2005).

[5] E. P. Samuel, M. P. Bhole, D. S. Patil, Semiconductor Science and Technology **21**, 993 (2006).

[6] E. P. Samuel, K. Talele, U. Zope, D. S. Patil, Optoelectronics and Advanced Materials-Rapid Communications **1**(5), 221 (2007).

[7] E. P. Samuel, D. S. Patil, Optoelectronics and Advanced Materials-Rapid Communications **1**(8), 394 (2007).

[8] Y. X. Liu, D. Z.-Y. Ting, T. C. McGill, Physical Review B **54**, 5675 (1996)

[9] C. Gmachl, D. L. Sivco, R. F.Colombelli, F. Capasso, A. Y. Cho, Letters to Nature **415**, 883 (2002).

[10] M. Bayer, A. Forchel, Physics Review B **65**, 41308 (2002).

[11] A. J. Williamson, L. W. Wang, Alex Zunger, Physical

Review B **62**, 12963 (2000).

[12] Towe Elias, Pan Dong, IEEE Journal of Selected Topics in Quantum Electronics **6**, 408 (2000).

[13] K. Matsuda, K. Ikeda, T. Saiki, H. Tsuchia, H. Saito, K. Nishi, Physical Review B **63**, 121304 (2001).

[14] N. Ledentsov Nikolai, M. Grundmann, F. Heinrichsdorff, Bimberg Dieter, V. M. Ustinov, A. E. Zhukov, M. V. Maximov, Zh. I. Alferov, J. A. Lott, IEEE Journal of Selected Topics in Quantum Electronics **6**, 439 (2000).

[15] T. Suski, G. Franssen, P. Perlin, R. Bohdan A. Bercha, P. Adamiec and F. Dybala, Applied Physics Letters, **84**, 1236 (2004).

[16] M. Gault, P. A. Mawby, M. S. Towers, IEE Proc. **140**, 44 (1993).

_____

[*]Corresponding author: patildsp@rediffmail.com